Space Charge and Electron Deflections in Beam Tetrode Theory

Part 2

By S. RODDA, B.Sc., F.Inst.P.*

6. Formation of a Virtual Cathode

IN order to explain what happens when a larger current is projected through the screen than can be transported to the anode it has to be supposed that a part of the current is reflected back to the screen. If the electrons are projected normally through the screen they could reverse their trajectories in the screen-to-anode space at a plane where the potential falls to zero, *i.e.*, if a "virtual cathode" were formed. At a virtual cathode a sorting action takes place, owing to the initial spread in velocities associated with thermionic emission, so that the fast electrons are transmitted to the anode and the slow electrons are reflected back to the screen. In the virtual cathode-to-screen space the returning electrons will add to the space charge density due to the forward electrons.

Let the virtual cathode plane be distant x_1 from the screen and x_2 from the anode; suppose that J_T = total current density projected through the screen and that J_A = current density reaching the anode. At the virtual cathode position dV/dx = zero and V = zero, as for a real cathode. (*See* Fig. 8.)

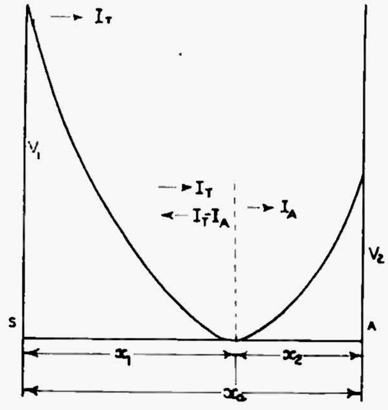

Fig. 8. Potential distribution when a virtual cathode is formed.

$$\text{Hence } x_1 = \sqrt{\frac{\left(\frac{2\epsilon}{m}\right)^{\frac{1}{2}}}{9\pi}}\;\frac{V_1^{3/4}}{\sqrt{2J_T - J_A}} \qquad (1)$$

as for a diode with space charge density due to the sum of J_T forward and $(J_T - J_A)$ back.

$$x_2 = \sqrt{\frac{\left(\frac{2\epsilon}{m}\right)^{\frac{1}{2}}}{9\pi}}\;\frac{V_2^{3/4}}{\sqrt{J_A}}$$

So that on summing:

$$x_1 + x_2 = x_a$$

$$= \sqrt{\frac{\left(\frac{2\epsilon}{m}\right)^{\frac{1}{2}}}{9\pi}}\left[\frac{V_1^{3/4}}{\sqrt{2J_T - J_A}} + \frac{V_2^{3/4}}{\sqrt{J_A}}\right] \qquad (2)$$

If this equation is rewritten in terms of "diode units" we get:

$$V_2^{3/4} = \sqrt{J_A} - \frac{\sqrt{J_A}}{\sqrt{2J_T - J_A}} \quad \ldots \quad (3)$$

If J_T is made infinitely large a rational solution is now given, $x_1 \rightarrow 0$, so that the virtual cathode is formed close to the screen and the limiting anode current is that of a diode of gap x_a and anode voltage V_2.

It is clear that in general V_2 and J_A will increase together from small values, but an examination of the Equation (3) shows that when $J_A = 2J_T - (2J_T)^{2/3}$ the slope of the J_A, V_2 curve is infinitely steep, and that for higher values of J_A the slope is negative, so that the J_A, V_2 curve begins to bend back. The corresponding value of V_2, denoted by V_σ at which the curve becomes infinitely steep is given by the relation:

$$W_\sigma = [(2J_T)^{1/3} - 1]^2 \quad \ldots\ldots \quad (4)$$

$$\text{where } W_\sigma = \frac{V_\sigma}{V_1}$$

It is supposed that the negative resistance region is unstable, and that it can be a cause of oscillations in a positive grid triode.[23] We may assume that when $V_2 = V_\sigma$ the anode current jumps to its full value J_T and that V_σ is therefore the "knee voltage" corresponding to V_2. This should be compared with the value:

$$W_K = [J_T^{1/3} - 1]^2$$

assigned to the "knee voltage" on Gill's theory.

The results of the two theories are shown by the curves of Fig. 9, in which J_A is plotted against the ratio V_2/V_1.

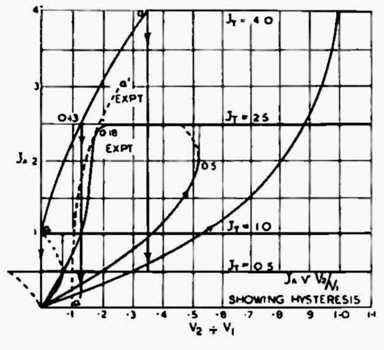

Fig. 9. J_A **plotted against** V_2/V_1.

Suppose, for example, we start with $J_T = 2.5$ units and a high value of anode voltage. As the anode voltage is reduced the anode current will be unaltered until the boundary curve aa is reached. The total current can no longer be fully transported, so that the system should jump to the virtual cathode mode and should remain in this until the anode voltage is raised above V_σ. The behaviour of the system is thus apparently characterised by an enormous hysteresis loop.

Unfortunately for the truth of the virtual cathode theory the quantitative agreement between the actual knee voltages and the calculated knee voltages is very poor—the calculated values are much too high.[24] For $J_T = 2.5$, W_σ is experimentally approximately 0.2 instead of 0.5 and therefore is nearer the limiting value set by the curve aa. As a consequence the hysteresis loops are not nearly so large as the synthesis of the virtual cathode theory and the Gill theory would indicate, although small loops can sometimes be demonstrated by taking dynamic characteristics on a cathode ray oscillograph, especially when the A-S gap is large.

Another difficulty is presented by both theories since they indicate that if I_T is low the value of W_k is zero. In practice, W_k follows the curve a'a' instead of aa, and is roughly 0.1 even at low projected current densities. It will be shown that these difficulties can be overcome if it is assumed that the electrons are not all projected normally through the screen but that they enter the screen-to-anode space over a range of angles to the normal.

A similar conclusion has already been drawn by Strutt and Van der Ziel in an important paper entitled "Über der Elektronen raumladung zwischen ebenen Elektroden, unter berucksichtigung der Anfangsgeschwindigkeit und Geschwindigkeitsverteilung der Elektronen," published in *Physica*, 1939,[25] if it is borne in mind that the velocity distribution of electrons projected into the S-A space arises from deflections at the grid and screen wires.

It would be an error to suppose that such a velocity distribution arises from the drop in potential between screen wire turns, except in so far as deflections are produced in the local fields around the wires. The field beyond the screen rapidly becomes uniform (unless the distance between adjacent turns is large) so that all electrons crossing a given plane will have the same total velocity, and they will therefore have the same forward velocities unless they have been deflected.

7.1. Electron Deflections

The rôle played by electron deflections in a positive grid triode, although referred to by Tonks, was first worked out by Below[26] who showed that the initial rising part of the I_A, V_2 characteristic could be ascribed to the effect of electron deflections at the grid. Consider a plane triode with grid at a positive potential V_1, and suppose that an electron enters the grid-to-anode space inclined at an angle θ_1 to the forward direction. If no further transverse forces act on the electron during its flight it will retain a constant transverse velocity. Hence if θ is the inclination of the electron trajectory at the plane where the potential is V, $V\sin^2\theta = \text{constant} = V_1\sin^2\theta_1$. At the position where the voltage V is $V_1\sin^2\theta_1$, θ will equal 90°, so that the electron will be brought to rest in the forward direction, and will begin to reverse its trajectory. The condition

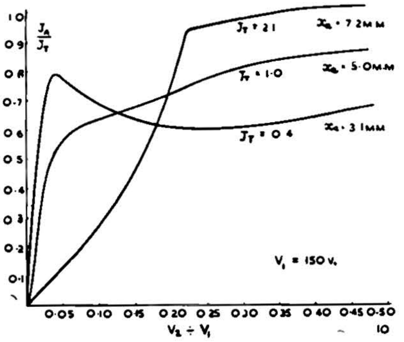

Fig. 10. Effect on characteristics of increasing relative space charge density, by increasing x_a.

in the plane case that an electron shall reach the anode is that there should be no potential between screen and anode lower than:

$$V_1\sin^2\theta_1$$

In a tetrode the same considerations apply if by V_1, θ_1 are understood the potential of the screen and the angle of entry of the electron into the S-A space.

θ_1 will, however, arise as the result of deflections by the control grid wires and by the screen grid wires. If, now, one could measure the primary current incident on the anode as a function of the potential minimum voltage V_m, the current collected will be due to those electrons whose deflections range from zero to $\sin^{-1}\sqrt{V_m/V_1}$: the more widely deflected electrons will be reflected back to the screen.

An immediate consequence of such a distribution-in-angle of the electrons projected into the S-A space is that the virtual cathode condition cannot be attained, since with a zero potential minimum all the electrons must surely be reflected. It is therefore necessary to modify the virtual cathode theory by postulating that V_m must be of sufficient height to transmit, at a given value of V_2, the observed anode current. Precisely the same mechanism is arrived at if it is considered that the initial rising part of the I_A/V_2 characteristic is a

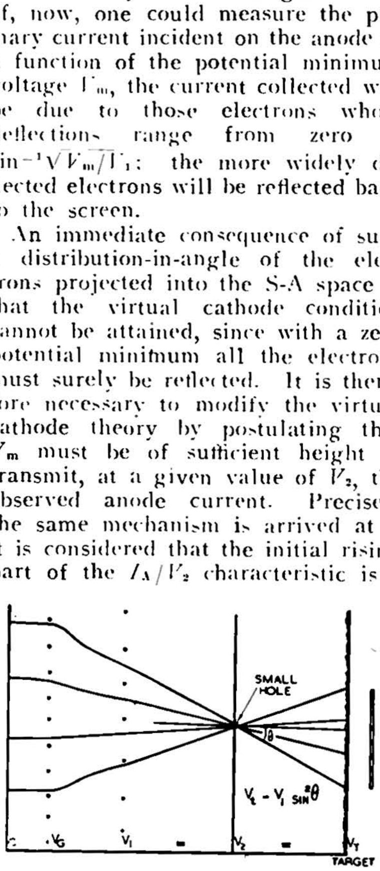

Fig. 11. Method of demonstrating deflections.

consequence of Below's theory[27] which must be modified by replacing the anode potential, V_2, by the potential minimum V_m produced by space charge. An experimental result which illustrates the effect of space charge is shown in Fig. 10, where a fixed current is projected into the S-A space. Since the screen and control grid voltages are kept constant the deflections of the electrons will be constant, except in so far as the deflections vary slightly with the electrostatic intensity on the anode side of the screen. If the S-A gap is made large the knee voltage greatly increases, but not to the value predicted by the virtual cathode theory ($W_\sigma = 0.36$ when $I_T = 2.1$).

In order to demonstrate the magnitude of electron deflections in actual valves the author has employed the simple method shown in Fig. 11.[28]

The anode of the tetrode has a small hole drilled in it. Electrons which emerge from the hole impinge on a fluorescent target. If the anode and the target are maintained at the same potential the electrons will travel in straight lines from the hole to the target. The results when current flows are indeed spectacular in that a long thin line appears on the target, showing that some electrons are greatly deflected in the plane normal to the grid and screen turns. (The fact that the line remains thin demonstrates that the effect cannot be due to space charge repulsion in the beam of the anode-to-target gap.) It is not essential that the anode should be kept at the target potential. If the potentials are unequal, the trajectories in the anode-target space will be parabolic.

It is a disadvantage with unequal screen, anode and target voltages that the hole will behave as an electrostatic lens. With a very small hole this is not serious except at low anode voltages.

Experiments show that the maximum angular deflection varies greatly with control grid voltage, as the following table shows:

V_1 = 135 volts		
V_g	$\sin^2\theta_1$	$V_1\sin\theta_1$
− 7.5	0.06	8.1
− 5.0	0.10	13.5
− 2.5	0.15	20.2
0.0	0.17	23.0
+15	0.06	8.1

Near cut-off the deflections are small; with bias approaching zero they rise to a maximum and then with increasing positive bias the deflections decrease again. This behaviour is what one would expect on electron optical considerations.

7.2. Deflection at the Control Grid

The simplest approach to the problem of calculating the deflections at the control grid is to suppose that the apertures between adjacent grid turns form cylindrical electron lenses. If the potential distribution is known, taking into account the presence of space charge, the precise trajectories can be determined step by step using Gabor's formula for the curvature:

$$\frac{1}{R} = \frac{\partial V / \partial n}{2V} \cos(\Psi - \theta)$$

The potential gradient $\partial V/\partial n$, makes an angle Ψ with the axis, and the normal to the electron trajectory an angle θ at a point where the potential is V. The co-ordinate system is taken with its axis a straight line normal to the grid plane passing midway between adjacent turns: the Y axis may be taken normal to this, in the grid plane.

When the control grid turns bear no charges the electrons are uninfluenced by the presence of the grid. The grid must then be at the (positive) potential V_t which would be found at the grid plane in the absence of the grid. When the control grid is at a negative potential the lens is convergent and the electrons are strongly deflected inwards towards the axis, but the beam cannot occupy the whole width between adjacent turns, since the electrons cannot come nearer a grid wire than to a zero equipotential. It seems reasonable to suppose that in this case the electron which has the maximum transverse velocity imparted to it is one which has been turned inwards from the zero equipotential and crosses the axis almost at right angles near the grid plane, where the potential is $\overline{V}$. Actually such an electron would swing across from one grid wire to the neighbourhood of the adjacent wire and be repelled inwards again, so that its transverse velocity is less than that acquired by falling through a potential difference $\overline{V}$. When the control grid is positive, the outer electrons are turned inwards from positive equipotentials. The maximum lateral velocity will therefore not exceed its value at zero grid bias, and for $V_g = V_t$ it will diminish to zero. Again, for bias values which are negative the transverse velocities must diminish, since $\overline{V}$ decreases. Finally, just at the point of cut-off when the emitting width

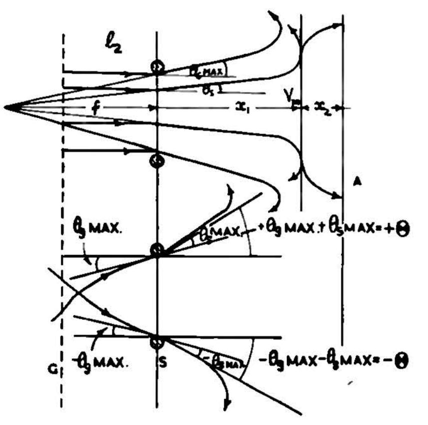

Fig. 12. Electron trajectories in neighbourhood of screen wires, showing divergent lens effect.

is zero, the beam width through the lens is so small that the extreme deflection becomes very small indeed.

It is interesting that instead of finding the trajectories in the actual system one can use a conformal transformation to a new geometrical system. The potential should at corresponding points be equal to that of the old system divided by the square of the modulus of transformation at the point considered. The new trajectories are the conformal transforms of the trajectories in the first system (Gabor[29]). The most convenient and practical method of examining the trajectories is to use the rubber drum model, which is illustrated, for example, in the paper by Jonker already referred to.

7.3. Deflection at the Screen

After an electron has escaped from the locally disturbed field near the grid plane its angle of inclination to the forward direction will decrease in such a way that $V\sin^2\theta$ remains constant. The value of θ when $V = V_1$ will be referred to as the reduced value of θ. At the screen there will be an additional angular deflection. (Fig. 12.)

Suppose that just before reaching the screen plane, the reduced angle of inclination is θ_g, due to deflection at the grid, and that the electron is given a further angular deflection θ_s near the screen wires. The total inclination after emergence from the screen plane will be $(\theta_g + \theta_s)$, so that the transverse velocity in electron volts:

$$V_t = V_1\sin^2(\theta_g + \theta_s) \approx V_1(\theta_g + \theta_s)^2 \quad (1)$$

if the angles are small. Thus if $\theta_s = \theta_g$ the overall value of V_t is four times the value attained at the control grid alone. At the screen Calbick's formula[30,31] for focal length f can be used, since the aberrations are small. An electron traversing the screen plane at a distance y from the axis of a lens will experience an angular deflection y/f radians. If we assume that the charge induced on the screen wires is mainly due to the electrostatic intensity in the control grid to screen space, then $f \approx 2l_2$ where l_2 is the grid-to-screen gap. Hence the value of θ_s is $y/2l_2$.

Let N_s = t.p.cm. of the screen winding; the maximum value of y, corresponding to an electron trajectory passing close to a screen wire, is $1/2N_s$, so that the maximum angular deflection is $1/4N_s l_2$ radians. As an example, let N_s = 10 t.p.cm., l_2 = 0.1 cm.:

$$\theta_{s\cdot max} = \frac{1}{4} \text{ radian}$$

When the grid and screen turns are aligned the beams transmitted through the control grid aperture will pass through the screen windings midway between the adjacent turns, and if the focusing action at the control grid is suitably contrived, the beam width at the screen plane will be relatively small; hence y is small, and the angular deflection is also small. If, however, the screen and grid turns are unaligned, y will have different values throughout the length of the tube, *i.e.*, y will depend on n where n is the aperture between the nth and $(n + 1)$th screen turns, counting from one end. Any value of y lying between $-1/2N_s$ and $+1/2N_s$ is equally likely, consequently, in summing up throughout the tube all the beam sections which enter the screen plane at an inclination θ_g, they will emerge over a range of angles lying between $\theta_g + \theta_{s\cdot max}$ and $\theta_g - \theta_{s\cdot max}$. Since θ_g can range in value from $-\theta_{g\cdot max}$ to $+\theta_{g\cdot max}$ the emergent electrons will range from: $-[\theta_{g\cdot max} + \theta_{s\cdot max}]$ to $+[\theta_{g\cdot max} + \theta_{s\cdot max}]$

Suppose that $I_g(\theta)$ represents the current transmitted through the grid with (reduced) angular deflection from $-\infty$ up to θ radians. Then, owing to the spreading out effect just described, the distribution-in-angle of the current leaving the screen plane will be:

$$I_s'(\theta_1) = \frac{1}{2\theta_{s\cdot max}} \int_{\theta_1 - \theta_{s\cdot max}}^{\theta_1 + \theta_{s\cdot max}} I'_g(\theta)d\theta \quad (2)$$

where $I_s(\theta_1)$ is the current transmitted through the screen with total angular deflections from $-\infty$ up to θ_1. $I_g'(\theta)$, $I_s'(\theta_1)$ are the differentials of $I_g(\theta)$, $I_s(\theta_1)$ with respect to θ and θ_1

respectively. The primary current reaching the anode will be equal to:

$$\int_{-\theta_1}^{+\theta_1} I_s'(\theta_1)d\theta_1$$

if limiting θ_1 is put equal to $\sin^{-1}\sqrt{V_m/V_1}$, *i.e.*, to $\sqrt{V_m/V_1}$ if V_m is small.

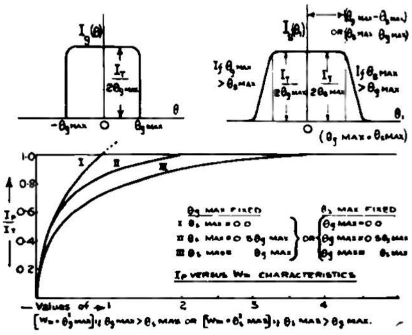

Fig. 13. Effect of deflections in modifying the anode current v. V_m/V_1 characteristic.

Now it is interesting to see that Equation 7.3.(2) converts a flat-topped rectangular distribution for $I_g'(\theta)$ into a trapezoidal distribution for $I_s'(\theta_1)$. Thus, although there is assumed to be a sudden jump to zero in $I_g'(\theta)$, there is no such sudden jump in $I_s'(\theta_1)$ and therefore there is no discontinuity in the slope of the anode current versus V_m characteristic, which could be supposed to correspond to a sharp knee voltage. This is illustrated in Fig. 13.

It is to be inferred, therefore, that because of cumulative deflections at the control grid and screen the maximum transverse velocity may be large, but at the same time the extremely deflected electrons are comparatively sparse, so that the I_A, V_m curve approaches the full current value gradually and without sudden changes in slope. The explanation of sharp " knees " must therefore lie in the properties of space charge.

(*To be concluded.*)

Bibliography

24 Harries, *Electronic Engineering*, Jan., 1942, p. 586.
25 Strutt & Van der Ziel, *Physica*, Oct., 1939, No. 9, p. 977.
26 Below, *Zeits. fur Fernmeldetechnik*, 1928, Vol. 9.
27 Harries, Rodda, *Wireless Eng.*, June, 1936, 13, p. 315.
28 Rodda, *Science Forum*, June, 1943.
29 Gabor, *Nature*, Dec. 5, 1942, p. 650.
30 Davisson & Calbick, *Phys. Rev.*, 38, 1931, p. 585.
31 Davisson & Calbick, *Phys. Rev.*, 42, 1932, p. 580.

Degassing of Light Metal Alloys by Sonic Vibrations

W. ESMARCH, T. ROMMEL and K. BENTHER

(W.V. Siemens Werke, Werkstoff Sonderheft, Berlin, 1940, pp. 78-87)

IT is well known that the passage of an ultrasonic wave in a liquid is accompanied by the formation of gas bubbles. These bubbles are partly due to the coalescence of microscopic bubbles already present in the liquid and are reinforced by previously dissolved gas being liberated in the low-pressure regions of the sound wave.

Kruger in 1931 took out a patent for degassing metallic melts by this method (German Patent No. 604486), ultra sonic waves being generated in the melt by a dipper controlled by a magnetostrictive oscillator. The main difficulty, in this process was the provision of suitable material for the dipper. Ceramic materials rapidly disintegrated while metallic dippers only proved suitable in rare instances. In addition the process of wave generation in the melt is very inefficient, a considerable proportion of the energy of the oscillator being lost by reflexion at the surfaces of separation or absorbed by the dipper.

It appears that the only way of making the process commercially possible would be the generation of high-frequency waves directly inside the melt. Now in the high-frequency electric furnace, the heat production is due to the formation of eddy currents in the charge. These eddy currents, moreover, are subjected to electrodynamic forces due to the magnetic field of the furnace circuit and cause the well-known rotary motion of the melt in induction furnaces.

This rotary motion favours the absorption of air by the molten material and therefore counteracts to some extent the degassing effect of the rise in temperature.

By superimposing a steady magnetic field on the high-frequency field of the furnace (the resultant field being in the direction of the coil axis) mechanical vibrations can be induced in the melt, the force at each point being proportional to the product of the local current density and field strength and acting radially to the coil axis. Moreover, by suitable choice of bath dimensions, resonance effects can be produced which increase the intensity of the vibrations.

We thus have a method of generating high-frequency waves in the melt without the need of a dipper. On the other hand, the frequency range is restricted to that of the alternating current feeding the furnace.

The authors are, however, convinced from preliminary experiments that there is no advantage from the degassing point of view of employing frequencies in excess of 10,000 sec., provided that the intensity of the vibration is sufficient.

In their experiments, therefore, an A.C. generator of this frequency was employed for feeding the furnace coil, the average current consumption being of the order of 100 A. The superimposed steady magnetic field was produced by 450 direct current fed with the same coil, the D.C. generator being protected by the insertion of suitable chokes and condensers. The total energy consumption amounted to about 15 kW, of which 10 kW were supplied by the high-frequency generator. With a specially designed heating coil, the energy consumption for the steady magnetic field could have been reduced very considerably.

The experiments were carried out with 8-10 Kg. melts of pure aluminium and aluminium-magnesium alloys, the temperature being kept constant at 700° C. Samples were drawn off every 10 minutes and the gas content determined by the well-known vacuum method.

It appears that alloys containing even relatively large per cent. of Mg can be completely degassed by this method in 30-60 minutes, provided the surface of the melt is protected by a fused salt layer and that dry air or nitrogen is directed on to the surface during the treatment.

Suitable salts can be obtained from the I.G. under the trade names Hydrosal and Elrasal. A laboratory product utilised by the authors and giving equally good results has the following composition:—

KCl	40 per cent.
$NaCl$	30 per cent.
$CaCO_3$	15 per cent.
NaF	15 per cent.

(*By courtesy of R.T.P. Section, M.A.P.*)